Dietary protein source mediates colitis pathogenesis through bacterial modulation of bile acids

Simon M. Gray[1*], Michael C. Wood[2*], Samantha C. Mulkeen[2], Sunjida Ahmed[2], Shrey D. Thaker[2], Bo Chen[2], William R. Sander[2], Vladimira Bibeva[2], Xiaoyue Zhang[3], Jie Yang[4], Jeremy W. Herzog[1], Shiying Zhang[5], Belgin Dogan[5], Kenneth W. Simpson[5], R. Balfour Sartor[1,6,7] and David C. Montrose[2,8]

[1]Center for Gastrointestinal Biology and Disease, Department of Medicine, University of North Carolina, Chapel Hill, NC

[2]Department of Pathology, Renaissance School of Medicine, Stony Brook University, Stony Brook, NY

[3]Biostatistical Consulting Core, Renaissance School of Medicine, Stony Brook University

[4]Department of Family, Population and Preventive Medicine, Stony Brook University, Stony Brook, NY

[5]Department of Clinical Sciences, Cornell University, Ithaca, NY

[6]Department of Microbiology and Immunology, University of North Carolina, Chapel Hill, NC

[7]National Gnotobiotic Rodent Resource Center, University of North Carolina, Chapel Hill, NC

[8]Stony Brook Cancer Center, Stony Brook, NY.

*Authors contributed equally.

Corresponding Author: David C. Montrose, Department of Pathology, Renaissance School of Medicine, Stony Brook University, MART Building, 9M-0816, Lauterbur Dr., Stony Brook, NY 11794. Phone: 631-216-2927; Fax: 631-444-3424; Email: david.montrose@stonybrookmedicine.edu

Keywords: Inflammatory bowel diseases; experimental colitis; dietary protein; beef; pea; interleukin-10 deficient mice; DSS; bile acids; microbiome

Funding: This work was supported by American Pulse Association and startup funds from the Stony Brook Cancer Center and Bahl Center for Metabolomics and Imaging (D.C.M.),

NIH/NIDDK T32DK007737 (S.M.G., R.B.S.), P01DK094779 (R.B.S.), P40OD010995 (R.B.S.), P30DK034987 (R.B.S.), Crohn's & Colitis Foundation Gnotobiotic Facility (R.B.S.), UNC Physician Scientist Training Program Fellowship Award (S.M.G.)

Declaration of interests:

D.C.M. has consulting arrangements with Gleipnir Medical. The authors have no other competing interests relevant to this study.

Acknowledgements

The authors thank members of the Montrose and Sartor laboratories for suggestions, helpful comments, and technical support. We thank Josh Frost, manager of the National Gnotobiotic Rodent Resource Center, and the Center staff members for gnotobiotic husbandry and mice. We acknowledge the Biological Mass Spectrometry Shared Resource at the Stony Brook Cancer Center for expert assistance with the MALDI-MS imaging analysis. We acknowledge the biostatistical consultation and support provided by the Biostatistical Consulting Core at School of Medicine, Stony Brook University.

Abstract

Evidence-based dietary recommendations for individuals with inflammatory bowel diseases (IBD) are limited. Red meat consumption is associated with increased IBD incidence and relapse in patients, suggesting that switching to a plant-based diet may limit gut inflammation. However, the mechanisms underlying the differential effects of these diets remain poorly understood. Feeding diets containing plant- or animal-derived proteins to murine colitis models revealed that mice given a beef protein (BP) diet exhibited the most severe colitis, while mice fed pea protein (PP) developed mild inflammation. The colitis-promoting effects of BP were microbially-mediated as determined by bacterial elimination or depletion and microbiota transplant studies. In the absence of colitis, BP-feeding reduced abundance of *Lactobacillus johnsonii* and *Turicibacter sanguinis* and expanded *Akkermansia muciniphila*, which localized to

53 the mucus in association with decreased mucus thickness and quality. BP-fed mice had
54 elevated primary and conjugated fecal bile acids (BAs), and taurocholic acid administration to
55 PP-fed mice worsened colitis. Dietary psyllium protected against BP-mediated inflammation,
56 restored BA-modulating commensals and normalized BA ratios. Collectively, these data suggest
57 that the protein component of red meat may be responsible, in part, for the colitis-promoting
58 effects of this food source and provide insight into dietary factors that may influence IBD
59 severity.
60

61 **Main Text**

62 Diet influences the pathogenesis and natural history of inflammatory bowel diseases
63 (IBD), disorders of chronic intestinal inflammation caused by dysregulated host immune
64 responses to resident intestinal microbes in genetically susceptible hosts[1-3]. Despite these
65 findings, limited evidence-based dietary recommendations exist to reduce the incidence and
66 severity of IBD[4-6]. For multiple decades IBD incidence has increased in the U.S. and globally,
67 including in regions with previously low rates[7-9]. Increased animal-based protein consumption,
68 including red meat, correlates with rising IBD incidence, suggesting a link between animal
69 protein consumption and IBD[10, 11]. However, the mechanisms by which specific dietary protein
70 sources promote gut inflammation remains unclear.

71 Diet regulates gut homeostasis and inflammation, in part, by shaping the composition,
72 function, and metabolic activity of the gut microbiota[2, 12-21]. For example, reducing dietary fiber or
73 increasing fructose consumption in mice enriches mucus-digesting resident bacteria, such as
74 *Akkermansia muciniphila*[12, 17-19, 21]. Further, consuming high fructose or dietary milk fat limits the
75 deconjugation of bile acids (BAs) (small molecules synthesized by the liver and modified by
76 intestinal microbes), resulting in increased levels of conjugated BAs (CBAs) and exacerbated
77 experimental colitis[17, 22]. Notably, patients with active IBD have higher levels of primary and
78 CBAs and depleted secondary unconjugated BAs, relative to healthy controls[23-25]. Moreover,

79 primary CBAs, which are metabolized by microbial enzymes to unconjugated secondary BAs,
80 exacerbate inflammation in experimental colitis models[22, 24, 26]. However, the role of dietary
81 protein source in these complex interactions and development of colonic inflammation is poorly
82 understood.

83 To investigate the impact of dietary protein source on experimental colitis severity, five
84 isocaloric synthetic diets containing protein isolates from beef, egg whites, casein, soy or pea
85 (**Table S1**) were fed to wild-type (WT) specific pathogen-free (SPF) C57BL/6J mice during
86 dextran sodium sulfate (DSS)-mediated induction of colitis. Mice fed beef protein (BP) diet
87 developed the most severe colitis while those fed pea protein (PP) diet developed the least
88 severe colitis; egg whites, casein, or soy protein diets induced intermediate colitis severity (**Fig.
89 1A-D**). BP feeding resulted in more severe colitis in a T-cell mediated colitis model using ex
90 germ-free (GF) *Il10*$^{-/-}$ mice colonized with mouse-adapted pooled human IBD microbiota (IMM-
91 HM2), to induce human IBD microbiota-associated colitis[27], compared to feeding a PP diet (**Fig.
92 1E-G)**. This was characterized by greater weight loss, more severe histologic inflammation and
93 higher expression of colonic pro-inflammatory cytokines (**Fig. 1E-G)**. Similar findings were made
94 in a second model of human IBD microbiota-associated colitis (IMM-g2)[27] (**Fig. 1H-J**). To
95 evaluate whether BP promotes colonic inflammation in the absence of a colitis inducer (i.e. DSS
96 or IBD patient-derived stool), WT SPF mice were fed standard chow, PP diet, or BP diet for 8
97 weeks and monitored, which showed no significant differences in DAI or colonic pro-
98 inflammatory cytokine expression **(Fig. S1A-B**). Collectively, these data demonstrate that the
99 protein component of beef worsens colonic inflammation in multiple experimental colitis models.

100 We next tested whether protein source modulates colitis severity, in part, through gut
101 resident bacteria. First, WT SPF mice were fed PP diet, BP diet, or BP diet in combination with
102 broad-spectrum antibiotics in drinking water to globally reduce gut bacteria, then challenged
103 with DSS while continuing the respective diets and antibiotics. Antibiotic treatment reduced BP
104 diet-mediated DSS colitis severity to, or below, PP diet-mediated levels (**Fig. 2A-C)**. An ~500-

105 fold depletion in total bacterial abundance in feces of mice given antibiotics was confirmed by
106 qRT-PCR. Next, GF *Il10*$^{-/-}$ mice were fed BP or PP diets for 14 days and assessed for colonic
107 inflammation by multiple parameters, which revealed no overt colitis in either group (**Fig. 2D-F**).
108 GF status in both groups was confirmed by anaerobic culture of feces (data not shown). Lastly,
109 we performed a fecal microbial transplant phenotype transfer experiment. Here, feces from WT
110 SPF mice fed BP or PP diets for 1 week were transplanted to GF WT mice fed standard rodent
111 chow and challenged with DSS for 10 days. Measurements of disease activity index (DAI),
112 colon length and histologic score showed that mice gavaged with fecal slurry from BP-fed mice
113 developed more severe colitis than mice administered feces from PP-fed mice (**Fig. 2G-I**).
114 Together, these data demonstrate that BP exacerbates colitis through the diet-altered
115 microbiota.

116 Since the dietary protein-altered microbiota mediates colitis severity, bacterial
117 community composition was profiled by 16S rRNA amplicon sequencing of feces from SPF WT
118 mice fed BP or PP diets for 1 week in the absence of colitis. Principal coordinates analysis
119 demonstrated distinct clustering of mice according to dietary protein source, which explained
120 approximately 65% of variation in the data (PERMANOVA test coefficient of determination, R^2 =
121 0.43, p=0.005) (**Fig 3A**). Although profiles before feeding either experimental diet were very
122 similar, 7 days of feeding BP or PP diet significantly altered the taxonomic abundance of
123 multiple bacteria (**Fig 3B; Fig. S2**). Significant expansion of *Akkermansia muciniphila* occurred
124 in the BP diet group, while *Turicibacter sanguinis* increased in the PP diet group, along with
125 preservation of *Lactobacillus johnsonii* (**Fig. 3B-C**). *A. muciniphila* can impair gut barrier function
126 through mucus digestion[12, 17, 21, 28-30], therefore, we examined its colonic luminal spatial
127 distribution by fluorescence *in situ* hybridization (FISH). This revealed high abundance of *A.*
128 *muciniphila* adjacent to the mucus layer of BP-fed mice while no signal was observed in PP-fed
129 mice (**Fig. 3D**). Colonic surface mucus thickness showed a corresponding ~50% reduction in
130 BP *vs*. PP fed mice (**Fig. 3E**). Additionally, surface mucus quality was reduced in BP- *vs*. PP-fed

131 mice with no obvious difference in goblet cell mucus staining (**Fig. 3F; Fig. S3**). To evaluate
132 whether BP-driven expansion of *A. muciniphila* was responsible, in part, for promoting colitis,
133 GF *Il10*$^{-/-}$ mice were selectively colonized with *A. muciniphila* alone, a consortium of IBD-
134 associated pathobionts including *Escherichia coli*, *Enterococcus faecalis*, and *Ruminococcus*
135 *gnavus* (EER), or *A. muciniphila* plus EER and fed BP diet. Although *A. muciniphila* mono-
136 association did not induce colitis, it significantly potentiated EER pathobiont-induced colitis
137 severity (**Fig 3G-H**). Appropriate strain colonization was confirmed by anaerobic plating of feces
138 from colonized mice followed by 16S colony PCR and Sanger sequencing of representative
139 colony morphologies (data not shown). These data suggest that BP exacerbates colitis, in part,
140 by promoting expansion of mucus-digesting *A. muciniphila* that potentiates the pro-inflammatory
141 effects of IBD-associated pathobionts.

142 Because bacteria have an important role in mediating BA metabolism and composition
143 and there was higher abundance of bile salt hydrolase (BSH)-carrying[31-34] bacteria (*T sanguinis*,
144 *L johnsonii*) in PP-fed mice, we next measured the relative levels of common BAs in feces from
145 WT SPF mice fed BP or PP diets for 7 days in the absence of colitis. This analysis showed that
146 most BAs in BP-fed mice were primary and conjugated while most BAs in PP fed mice were
147 secondary and unconjugated (**Fig. 4A**). Multiple taurine conjugated primary BAs, including
148 taurocholic acid (TCA), were significantly higher in BP-fed mice while several unconjugated
149 secondary BAs, including lithocholic acid (LCA) and deoxycholic acid (DCA), were elevated in
150 PP-fed mice (**Fig. 4B**). These patterns were not observed in the livers or ileal content of mice
151 fed BP *vs*. PP diets (data not shown), suggesting that fecal BA alterations are likely mediated by
152 colon-specific microbial differences. To connect the respective BA profiles of mice fed PP or BP
153 diets with differential bacterial abundance, we performed an *in vitro* bile acid deconjugation
154 assay comparing select bacterial species enriched by either diet. This revealed that *L. johnsonii*
155 (higher abundance in PP-fed mice) deconjugated TCA to cholic acid (CA) 100-fold more than *A.*
156 *muciniphila* (increased in BP-fed mice) (**Fig. 4C**). To evaluate whether the primary CBAs that

157 were increased in feces of BP diet-fed mice directly exacerbate colitis, PP-fed mice were
158 administered TCA by oral gavage daily for 7 days and exposed to DSS. DAI, colon length and
159 histologic score showed that TCA worsened colitis in PP-fed mice (**Fig 4D-F**). Subsequent
160 MALDI-MSI based imaging of the colon of mice administered TCA in the absence of colitis
161 revealed TCA accumulation in the colonic epithelium (**Fig. S4**). Collectively, these data suggest
162 that mice consuming a BP-containing diet have lower abundance of BA-deconjugating bacteria,
163 resulting in higher levels of colitis-promoting primary CBAs.

164 Microbe-accessible dietary fiber supports populations of gut health-promoting
165 commensals, including BA-metabolizing bacteria[35]. Therefore, we reasoned that maintaining
166 these bacterial populations by adding soluble dietary fiber would attenuate BP-driven colitis
167 severity. To test this concept, ex-GF *Il10*$^{-/-}$ mice inoculated with MA human IBD microbiota were
168 fed PP diet, BP diet, or BP diet in which cellulose fiber was replaced with psyllium (BP-psyllium
169 diet) and monitored for colitis severity (**Table S1**). Compared to BP diet, the BP-psyllium diet
170 significantly decreased colitis severity, as determined by body weight, fecal lipocalin, histologic
171 analysis and cytokine gene expression (**Fig. 4G-J**). Similar protection by psyllium was observed
172 in the DSS-induced colitis model (**Fig. S5**). Analysis of BA-metabolizing bacteria and BA profiles
173 in WT C57BL/6J mice fed each of these three diets in the absence of colitis showed that
174 psyllium supplementation significantly increased the relative abundance of *L. johnsonii* and the
175 CA:TCA ratio in BP-fed mice (**Fig. 4K-L**). Taken together, these data support a model in which
176 BP-exacerbated colitis, which is driven by high abundance of primary CBAs, can be attenuated
177 through psyllium fiber administration, restoring populations of BSH-carrying bacteria that convert
178 primary CBAs to their deconjugated form.

179 Plant-based diets are believed to benefit IBD patients, while animal-based diets may be
180 detrimental. Both retrospective and prospective studies suggest that consumption of red meat is
181 associated with IBD incidence and disease activity. For example, The E3N Prospective Cohort
182 Study revealed that high animal protein consumption significantly increased IBD incidence[36] and

183 multiple studies showed that meat intake increased the risk of disease flare in patients with
184 ulcerative colitis (UC)[5, 37, 38]. The concept that plant-based diets are beneficial largely stems from
185 studies demonstrating that microbe-fermentable carbohydrates from plants reduce experimental
186 colitis[2, 39]. In contrast, diets rich in animal-derived products (especially red meat) are thought to
187 promote intestinal inflammation through heme, sulfur and saturated fat content[2, 39]. Although
188 these components of plant and animal-based diets impact gut health, the role of protein content
189 has not been widely considered. Our study, which selectively examined protein content by
190 feeding mice identical diets except for the type of protein isolate, suggests that the source of
191 dietary protein content differentially impacts colitis severity. Other studies investigating the
192 impact of protein source on experimental colitis, including from beef and pea, are largely
193 consistent with the data shown in the current study, although this previous work used diets
194 containing whole food sources rather than purified protein isolate[14, 15, 40, 41]. Our findings support
195 a role for the dietary protein-altered microbiota and BAs in mediating colitis severity, however,
196 the specific mechanism(s) by which protein type drives these effects remains unclear. It is
197 plausible that differences in amino acid composition or digestion/absorption of diverse dietary
198 protein sources are contributing factors. Therefore, determining which amino acids or what
199 properties of each protein type mediate intestinal inflammation will be important for future
200 studies.

201 Bacteria, BAs and their interplay are key mediators of IBD pathogenesis[1, 2]. Higher levels
202 of conjugated and primary BAs are found in feces of patients with active IBD, compared to
203 unconjugated and secondary BAs in healthy individuals[23-25]. Our work suggests that a shift to a
204 predominance of conjugated and primary BAs, is in part, responsible for greater colitis severity
205 when feeding BP to mice. We found that taurine conjugated and primary BAs are higher in BP-
206 fed mice than PP-fed mice, and showed that direct administration of TCA, which was highly
207 increased in the BP-fed group, worsened colitis in PP-fed mice to levels observed in mice given
208 BP diet alone. Although the exact mechanism(s) by which altered BAs enhance disease is

209 unclear, the detergent-like properties of BAs could disrupt gut barrier function by impairing
210 epithelial cell function and/or epithelial-protective mucus. This concept is supported by our data
211 showing the ability of exogenously administered TCA to localize to the colonic epithelium.
212 Interestingly, our prior work showed that a high fructose diet exacerbated murine colitis with a
213 similar increase in CBAs as observed in BP fed mice, with rectal administration of CBAs
214 worsening colitis and thinning colonic mucus in mice fed a control diet[17]. Integrating our study
215 focused on dietary protein with prior studies of the role of dietary fat and carbohydrates in
216 experimental colitis suggests that altered BAs may be a common pathway for diet-mediated gut
217 inflammation[17, 22]. Although our work focused on the detrimental impact of conjugated primary
218 bile acids enriched in BP-fed mice, the profile of unconjugated, secondary bile acids enriched in
219 feces from PP fed mice might itself be protective. For example, LCA and DCA, both enriched in
220 PP-fed mice, are strong ligands of the PXR and TGR5 receptors that, when activated, induce
221 anti-inflammatory effects[24, 42-44]. Therefore, the role of unconjugated secondary bile acids as
222 protective metabolites in PP-fed mice is an important future direction.

223 Bile acids have a bidirectional relationship with gut bacteria, whereby bacterial enzymes
224 metabolize BAs, which in turn, alter bacterial physiology and microbiota composition[42]. PP
225 feeding expanded bacterial species that efficiently deconjugate BAs, including *L johnsonii* and *T*
226 *sanguinis* (as shown by data from the deconjugation assay performed in the current study and
227 previous work[32]), while BP feeding expanded *A muciniphila,* a poor deconjugator that also
228 degrades mucus and potentiates pathobiont-driven inflammation[45]. These dietary protein-
229 induced bacterial shifts likely caused the observed BA profiles, however, we cannot exclude the
230 possibility that altered BAs directly shifted microbiota composition, as previously
231 demonstrated[46-49]. Further evidence that the ratio of conjugated to unconjugated BAs are
232 important for mediating colitis stems from our findings that psyllium supplementation protected
233 against BP-mediated colitis severity, while maintaining favorable BA profiles and populations of
234 BA-deconjugating bacteria. However, psyllium fiber likely protects against inflammation by

235 multiple mechanisms, including SCFA production and prevention of bacterial mucus
236 degradation[12, 50].
237 Our study reaffirms the concept that IBD occurs when multiple detrimental factors
238 intersect to initiate and perpetuate gut inflammation[51]. These IBD determinants – genetically
239 dysregulated host inflammatory and epithelial barrier responses, abnormal resident microbes,
240 and environmental triggers – can exist in isolation or combination without causing disease, but
241 together drive severe IBD. For example, GF colitis susceptible *Il10*$^{-/-}$ mice fed BP diet (genetic
242 susceptibility + environmental trigger) did not develop inflammation, nor did SPF WT mice fed
243 BP-diet (resident microbes + environmental trigger). However, we demonstrated that when all
244 three IBD-driving factors – host, microbe, and environment – intersect, severe and progressive
245 intestinal inflammation occurs. The poor long-term success of current human IBD therapies may
246 reflect a failure to reconcile the multiple determinants of IBD. For example, addressing just one
247 factor, such as suppression of host inflammation, leaves the patient vulnerable to recurrent
248 disease upon encountering environmental triggers. We suggest that durable long-term
249 remission requires simultaneously addressing all IBD determinants, and as such, investigations
250 into environmental drivers of IBD, especially diet, is required to guide clinical approaches to
251 maintain sustained remission.
252
253 **Methods**
254 *Murine colitis models*
255 To induce chemical colitis, 8-week-old male C57BL/6J mice (The Jackson Laboratory)
256 were administered 1% DSS (Sigma) in drinking water for 6–7 days, as indicated. Colitis severity
257 was assessed by measuring changes in body weight, as well as severity of rectal bleeding and
258 diarrhea, as previously described[17, 52]. Disease Activity Index (DAI) was calculated by combining
259 severity of body weight loss, diarrhea and bleeding, as previously described[17, 52].

260 T cell-mediated colitis was induced by inoculation of mouse-adapted human IBD patient
261 fecal microbiota (previously developed and characterized[27]) to GF *Il10*$^{-/-}$ mice on a 129S6/SvEv
262 background (purchased from the National Gnotobiotic Rodent Resource Center (NGRRC) at the
263 University of North Carolina), as previously described[27]. Mouse-adapted (MA) human IBD
264 patient microbiota was previously generated from de-identified human IBD patient stool samples
265 collected under an Institutional Review Board approved protocol; no primary human samples
266 were used in this study[27]. Briefly, human fecal materials from pooled cohorts of human donors
267 with active IBD were passaged through GF 129S6/SvEv *Il10*$^{-/-}$ mice to generate standardized
268 aliquots of fecal slurry[27]. MA IMM-g2 microbiota was derived from pooled feces of 2 CD and 1
269 UC patient and MA IMM-HM2 microbiota was derived from pooled feces of 3 CD patients[27].
270 Standardized 100mg/ml aliquots of mouse-adapted human IBD microbiota were anaerobically
271 thawed, diluted with pre-reduced PBS, and administered by oral gavage (2mg) to recipient GF
272 *Il10*$^{-/-}$ mice[27]. All fecal transplant experiments were performed with sterile gnotobiotic cage
273 technique in BSL-2 isolation cubicles with HEPA-filtered air[53]. Prior to colonization, GF mice
274 were fed Purina Advanced Protocol Select Rodent 50 IF/6F Auto Diet. Defined diets were
275 started at the time of fecal microbiota transplant.
276 At the end of the experimental periods, mice were humanely euthanized using CO_2.
277 Excised colons were measured then flushed with ice-cold phosphate-buffered saline (PBS).
278 Tissue was either snap-frozen for biochemical analysis or fixed in 4% paraformaldehyde or 10%
279 phosphate buffered formalin for 4-24 hours, followed by paraffin embedding and H&E staining
280 for histological analysis. All animal studies were approved by the Institutional Animal Care and
281 Use Committee at Stony Brook University and the University of North Carolina at Chapel Hill.
282
283 *Diet-polarized fecal microbiota transplant (FMT)*
284 Feces were collected from WT C57BL/6J SPF mice fed BP or PP diets for 2 weeks,
285 anaerobically homogenized, and diluted in pre-reduced lysogeny broth (LB) with 20% glycerol to

286 generate fecal slurries (n=5-6 donor mice per diet). Each donor FMT was administered to 1-2
287 recipient mice GF C57BL/6J mice via oral gavage on days 0, 3, 5, 7, and 9 of the experiment.
288 Mice were administered 2% DSS from days 3-10 of the experiment and monitored for signs of
289 colitis.
290
291 *Inoculation of defined consortia*
292 *Escherichia coli* LF82[54], *Enterococcus faecalis* OG1RF[55], and *Ruminococcus gnavus*
293 ATCC 29149[55] (EER) were grown under anaerobic conditions in brain-heart infusion medium
294 supplemented with 5g/L yeast extract, 0.5g/L L-cysteine, and 5mg/L hemin (LYH-BHI medium).
295 *A. muciniphila* ATCC BAA-835 (AM) was grown under anaerobic conditions in LYH-BHI medium
296 supplemented with 5g/L porcine gastric mucin (LYH-BHI + PGM). Pure cultures of each strain
297 were grown anaerobically to confluence then equally mixed to generate EER or EER + AM
298 consortia. GF 129S6/SvEv *Il10*$^{-/-}$ mice were colonized with freshly cultured consortia by oral
299 gavage and given BP diet from the time of colonization. Feces were collected at necropsy, serial
300 diluted and plated under anaerobic conditions on LYH-BHI + PGM to confirm colonization with
301 consortia members. Representative colonies of each strain identified by colony morphology
302 were picked from plates, 16S PCR amplified, and Sanger sequenced (Eton Bioscience) to
303 confirm colonization of appropriate strains in recipient mice.
304
305 *Histopathologic scoring*
306 Colons from mice given DSS were flushed, formalin fixed, and paraffin embedded
307 followed by sectioning and staining with hematoxylin and eosin. Scoring of colitis/colonic
308 inflammation was performed based on evaluation of mucosal damage by acute inflammation, by
309 crypt abscess, mucosal architectural distortion and proportion of the involvement of colon as
310 previously described[56]. Briefly, epithelial damage by acute inflammation was graded into 4
311 categories (0-3; 0=no inflammation. 1=mild, 2=moderate and 3=severe inflammation with

312 ulceration). Mucosal damage with crypt abscess graded into 2 categories (0=absent and
313 1=present). Extent of acute inflammation was graded into 4 categories (0-3; 0=no inflammation,
314 1=mucosal, 2=submucosal and 3=transmural). Mucosal architectural distortion was graded into
315 4 categories which includes the percentage of length of colon involvement (0-3; 0=normal
316 architecture, 1= mild/focal or 10%, 2=moderate/20-30%, and 3=severe/ >40% of the entire
317 length). Proportion of the total involvement was evaluated by the percentage of length of colon
318 involved by colitis into 4 categories (0-3; 0=no colitis, 1=1-10% of the total length, 2=20-30%
319 and 3=>40% of the total evaluated length of colon). All histologic scoring was performed in a
320 blinded fashion by a board-certified gastrointestinal pathologist (S.A.).

321 For *Il10*$^{-/-}$ experimental colitis studies, histologic inflammation was quantified in ileal,
322 cecal and colonic (proximal, distal, rectal) tissue segments using a well-validated rubric by
323 blinded histopathology scoring on a scale of 0-4 for each segment, as previously described[27, 56,
324 57]. Total histology score was calculated by summation of all 5 tissue segment scores for a scale
325 of 0-20.

326

327 *Fecal lipocalin-2 quantification*

328 Fecal samples were homogenized in PBS with 0.1% Tween 20, incubated at 4°C for 12
329 hours, then centrifuged to yield clear supernatant for lipocalin-2 ELISA, performed according to
330 the manufacturer's instructions (DY1857, R&D Systems)[58].

331

332 *Measurements of mucus thickness and quality*

333 Segments of harvested colons from mice containing a fecal pellet were preserved in
334 fresh Carnoy's fixative solution (methanol:chloroform:glacial acetic acid, 60:30:10) then
335 sequentially washed in methanol, ethanol and xylenes, as previously described[17]. Tissues were
336 then paraffin-embedded and sectioned (5 μm), followed by staining with Alcian Blue, and mucus

337 thickness was measured in 20-50 regions of each colon in a blinded manner using ImageJ
338 software (National Institutes of Health, Bethesda, MD), as previously described[17].
339 To determine differences in mucus quality on the surface of the epithelium and within
340 goblet cells, Periodic acid Schiff (PAS) staining was performed. Stained slides were scanned
341 using an Aperio Image Scope (ScanScope, Aperio, CA) and used to count the PAS-positive
342 pixels by the Aperio Color Deconvolution algorithm, as previously described[17].
343
344 *qRT-PCR*
345 For measurements of mammalian gene expression, RNA was isolated from tissues
346 using QIAzol Lysis Reagent (Qiagen) following the manufacturer's protocol. RNA concentration
347 was measured using a NanoDrop ND-1000 spectrophotometer. cDNA was synthesized using
348 2000 ng total RNA and reverse transcriptase qScript SuperMix (Quanta). Quantitative real-time
349 PCR was performed using specific primers on a QuantStudio 7 Real-Time PCR System
350 (Applied Biosystems) using PowerTrack SYBR Green PCR Master Mix and oligo (dT) primers
351 according to the user's manual. *Actb* expression was used as internal control for gene
352 expression. The ΔΔCT method was used to calculate relative fold expression. Primer
353 sequences are shown in **Table S2**.
354 For bacterial abundance and bacterial gene expression analysis, DNA was extracted
355 from fecal samples using the QIAamp DNA Fast Stool Mini Kit (Qiagen) per the manufacturer's
356 instructions. For each sample, 10 ng of DNA was used for qRT-PCR using PowerTrack SYBR
357 green PCR master mix on a QuantStudio 7 PCR Machine. Bacterial primers sequences are
358 shown in **Table S2**. Relative abundance was calculated by the ΔΔCT method using universal
359 16S primers as control.
360
361 *Bile acid analysis*
362 Fecal and ileal samples were dried in a vacuum centrifuge then homogenized in 500 μL

363 of cold 80% methanol. Liver samples were homogenized using the same method but without
364 prior drying. Bacterial supernatants were mixed with cold 80% methanol in a 1:9 ratio. Following
365 homogenization or mixing, samples were centrifuged at 14,000 rcf for 20 minutes at 4°C and the
366 supernatant was collected and dried down using a vacuum centrifuge then stored at -80° C prior
367 to analysis. Bile Acid analysis was performed as previously described on a Vanquish UHPLC
368 system coupled to a Q Exactive Orbitrap mass spectrometer (Thermo Scientific)[17].
369 Relative quantitation was normalized to dry weight of fecal/ileal samples or protein
370 concentration of livers. Analysis was performed at the Proteomics & Metabolomics Core Facility
371 of Weill Cornell Medicine.
372
373 *MALDI Mass Spectrometry Imaging*
374 Tissue preparation and imaging was performed following a previously published
375 method[59]. Briefly, mouse colons were processed into Swiss-rolls, embedded in 5%
376 carboxymethylcellulose, and stored at -20°C. Serial frozen sectioning was performed for paired
377 MALDI imaging and standard H&E staining. MALDI imaging was conducted on a rapifleX mass
378 spectrometer (Bruker Daltonics) within metabolite mass range in negative ion detect mode at 50
379 µm spatial resolution. The TCA deprotonated ion with a mass-to-charge ratio of 514.284 m/z
380 was detected, and the average intensity of the mass spectrometry signal for TCA determined
381 using SCiLS Lab software (Bruker Daltronics).
382
383 *16S rRNA Analysis*
384 Frozen fecal samples were shipped to Molecular Research (Shallowater, TX) for 16S
385 rRNA profiling, performed as previously described[17]. DNA was extracted with the Powersoil
386 DNA Kit (Qiagen). The 16S rRNA gene V4 variable region was targeted for PCR amplification,
387 followed by Illumina HiSeq short-read sequencing. Sequencing outputs were processed and
388 taxonomically classified as previously described[17]. Operational taxonomic units were defined by

389 clustering at 97% similarity (3% divergence) and classified by BLASTn against an RDPII/NCBI
390 derived database. Statistical analysis and visualization of principal coordinates analysis (PCoA)
391 plots were performed with the Shiny application *Plotmicrobiome* (Sun et al. GitHub
392 https://github.com/ssun6/plotmicrobiome).
393
394 *Fluorescence in situ hybridization (FISH)*
395 Fluorescence in situ hybridization (FISH) was performed as previously described[17, 60] on
396 4μm histologic sections of Carnoy's-fixed paraffin-embedded colon tissue using an *A.*
397 *muciniphila*-specific FISH probe (S-SMUC-1437-a-A-20: Cy-3-50-
398 CCTTGCGGTTGGCTTCAGAT-30)[17, 60]. Slides spotted with multiple control bacteria (*E. coli, P*
399 *vulgaris, K pneumoniae, S equi, S bovis*) not-reactive to the A.M. FISH probe were used to
400 confirm probe specificity[17, 60].
401
402 *In vitro bacterial culture and treatment*
403 *L. johnsonii* BAA-3147 and *A. muciniphila* BAA-835 from frozen stocks were cultured
404 overnight in MRS or LYH-BHI + 0.5% mucin, respectively, the day before the experiments. *A.*
405 *muciniphila* BAA-835 was cultured in an anaerobic chamber (Coy Laboratory) with mixed gas
406 (90% N2, 5% CO2 and 5% H2; 37°C), and *L. johnsonii* BAA-3147 was cultured under aerobic
407 conditions (37°C with shaking at 150 rpm). The overnight cultures were diluted with fresh media
408 with or without 1 mM taurocholate to *A. muciniphilla* BAA-835 (once at OD600 of 1-1.1) and to
409 *L. johnsonii* (once at OD600 of 0.7-0.8). The diluted cultures were immediately distributed into
410 two sets of tubes for 0 and 24 h time points, each in triplicate. The time 0 h samples were
411 transferred to ice immediately to prevent bacterial activity on taurocholate. Optical densities
412 were measured at each time point for normalization. The cultures were then centrifuged at
413 3,000 rpm for 20 min at 4°C and the supernatants were filtered through a 0.2 μm syringe filter
414 and kept at -80°C until BA measurements.

415

416 *Statistical analysis*

417 For the comparison of DAI across different mice groups, linear mixed-effects models for
418 longitudinal data analysis were used. Model assumption was confirmed using residual
419 diagnosis. Time (in days) was treated as a continuous variable to assess the trend in DAI. An
420 interaction term between diet group and time was used to compare the trends across groups.
421 The covariance structure used to model the correlated longitudinal measurements from the
422 same mice was unstructured (UN), selected based on Akaike Information Criterion (AIC) from a
423 set of possible structures. For the comparison of numeric values observed or calculated at the
424 end of experiments, Wilcoxon rank-sum tests or simple linear regression models were used.
425 These analyses were applied to the following variables: % body weight change, histology score,
426 gene expression, colon length, bacterial abundance, mucus thickness, mucus quality, and bile
427 acid ratios. A P-value less than 0.05 was considered statistically significant and analyses were
428 performed using SAS 9.4 (SAS Institute Inc., Cary, NC).

429 Statistical analysis of BA levels. The BA dataset was filtered to remove BA with >50%
430 missing values. Normalization of raw metabolite levels was performed by probabilistic quotient
431 normalization followed by log2-transformation and imputation of missing values by k-nearest
432 neighbor (KNN). BA differences were quantified by log2 fold change from the PP diet group.
433 Linear models with diet as the independent variable were used to calculate statistical
434 significance. The Benjamini-Hochberg method with an FDR cut-off of 0.2 was used for multiple
435 hypothesis correction. Analyses were performed with the maplet package (version 1.2.1) in R [61].

436

437 **Figure Legends**

438 **Figure 1. Dietary beef protein worsens murine colitis compared to other protein sources**
439 A-D, C57BL/6 mice were fed isocaloric diets containing protein isolate derived from beef (BP),
440 soy (SP), egg whites (EP), casein (CP), or pea (PP) for 7 days, followed by administration of 1%

441 DSS for 7 days, while being continued on the respective diets. Disease activity index (DAI) was
442 measured during DSS exposure (A), percent of body weight change relative to day 0 of DSS
443 exposure was calculated following 7 days of DSS administration (B) and histologic score was
444 assessed in colons on day 7 of DSS administration (C). n = 6 mice per group. Representative
445 histologic images of colons from BP or PP-fed mice are shown (D). E-G, germ-free *Il10*$^{-/-}$ mice
446 were inoculated with mouse-adapted (MA) pooled human IBD patient fecal microbiota (IMM-
447 HM2) then fed diets containing BP or PP for 14 days. Weight change relative to day 0 was
448 measured (E), representative histologic images of colons are shown (left side) and total
449 histology score was assessed (right side) (F), and relative gene expression of cytokines were
450 measured in colons (G), on day 14. n = 7-8 mice per group. H-J, germ-free *Il10*$^{-/-}$ mice were
451 inoculated with a second MA pooled human IBD patient fecal microbiota (IMM-g2) then fed BP
452 or PP diets for 8 days. Weight changes relative to day 0 were measured (H), representative
453 histologic images of colons are shown (left side) and rectal histology score was assessed (right
454 side) (I), and relative gene expression of cytokines were measured in colons (J), on day 8. n =
455 4-6 mice per group. Data representative of 3 (E-G), and 3 (H-J) independent experiments.
456 *P<0.05; **P<0.01; ***P<0.001; ****P<0.0001. Bar plots show mean and standard deviation.
457

458 **Figure 2. Gut bacteria are causally linked to beef protein-worsening of colitis**

459 A-C, C57BL/6J mice were fed beef protein (BP) or pea protein (PP)-containing diets or beef
460 protein diet and administered a five-antibiotic cocktail (ampicillin, gentamicin, metronidazole,
461 neomycin, vancomycin[17]) in drinking water for 14 days (BP + Abx), then all mice were given 1%
462 DSS in drinking water for 7 days while being continued on control or antibiotics-containing
463 water. Disease Activity Index (DAI) was measured during DSS exposure (A), colon length was
464 measured on day 7 (B) and histologic inflammation of colons was assessed on day 7 (C). n = 8
465 mice per group. D-F, germ-free *Il10*$^{-/-}$ mice were fed sterile BP or PP diets for 14 days.
466 Representative histologic images of colons are shown (D), histology score was assessed (E)

467 and relative gene expression of *Il1b* was measured in colons (F), on day 14. n = 4-5 mice per
468 group. G-I, germ-free wild-type mice were inoculated with colonic luminal fecal contents of
469 specific pathogen-free mice fed BP or PP diets for 7 days. Recipient mice were then fed
470 standard chow and administered 1% DSS for 7 days and DAI was calculated (G), colon length
471 was measured (H) and histologic inflammation of colons was assessed (I), on day 10. n = 9-10
472 per group; data are representative of 2 independent experiments. *P<0.05; **P<0.01;
473 ***P<0.001; ****P<0.0001. Bar plots show mean and standard deviation.
474
475 **Figure 3. Beef protein consumption promotes *A. muciniphila* expansion and gut barrier**
476 **defects**
477 A-C, C57BL/6J mice were fed either beef protein (BP) or pea protein (PP)-containing diets for 7
478 days then fecal samples were subjected to 16S rRNA sequencing. Results are displayed as
479 principal coordinate analysis on day 7 (A) and as percent abundance of each species on days 0
480 and 7 (B) (those species <1% in overall abundance are labeled as 'Other'). qRT-PCR was
481 performed on fecal DNA to measure relative abundance of major populations found in either diet
482 group (C). D-F, C57BL/6J wild-type mice were fed BP or PP diets for 7 days then colons were
483 harvested and fixed to preserve the mucus layer. Fluorescence *in situ* hybridization was
484 performed to identify *A. muciniphila* (indicated by orange structures) (D), Alcian blue staining
485 was carried out to measure mucus thickness (representative images shown on left side and
486 quantification of staining shown on right side; bracket indicates mucus layer on images) (E), and
487 periodic acid Schiff staining was performed to quantify mucus quality (representative images
488 shown on left side and quantification of staining shown on right side) (F). n = 6 per group. G-H,
489 germ-free *Il10*$^{-/-}$ mice were inoculated with *A. muciniphila*, a defined consortium of *Escherichia*
490 *coli*, *Enterococcus faecalis*, and *Ruminococcus gnavus* alone or in combination with *A.*
491 *muciniphila* and fed BP diet. Representative histologic images of ceca are shown (left side) and
492 total histology score was assessed (right side) (G) and relative expression of inflammatory

493 cytokine genes was measured (H) in the ceca of mice on day 14. n = 7-9 per group, data
494 representative of 2 independent experiments. *P<0.05; **P<0.01; ***P<0.001; ****P<0.0001. Bar
495 plots show mean and standard deviation.
496
497 **Figure 4. Bacteria-mediated bile acid changes facilitate colitis severity**
498 A-B, WT C57BL/6J mice were fed diets containing either beef protein (BP) or pea protein (PP)-
499 containing diets for 7 days and the relative abundance of bile acids was measured in feces. The
500 average percent of primary *vs*. secondary or conjugated *vs*. unconjugated bile acids in each diet
501 group is shown (A) and those BAs that displayed significantly different abundance (FDR<0.1)
502 are shown as log2 fold-change in PP-fed mice relative to BP-fed mice (B). C, taurocholic acid
503 (TCA) (1mM) was administered to culture medium of *L. johnsonii* and *A. muciniphila* and the
504 levels of cholic acid were measured in the supernatants after 24 hours and reported as relative
505 to either species cultured in the absence of TCA. D-F, C57BL/6J WT mice were fed either BP or
506 PP diets and given daily oral gavage of PBS or fed PP and gavaged daily with TCA (0.35mg/kg)
507 for 7 days, then administered 1% DSS in drinking water for 7 days, while continuing oral
508 administration. Disease Activity Index (DAI) was measured over 7 days (D), colon length was
509 measured on day 7 (E) and histologic inflammation of colons was assessed on day 7 (F). G-J,
510 germ-free *Il10*$^{-/-}$ mice were inoculated with mouse-adapted pooled human IBD patient fecal
511 microbiota (IMM-HM2) then fed BP or PP diets containing cellulose or BP diet containing
512 psyllium (BP + psyllium) for 14 days. Weight changes relative to day 0 were calculated (G),
513 fecal lipocalin-2 (f-Lcn) was measured (H), total histology score was assessed (I), and relative
514 gene expression of inflammatory cytokines in colons was measured (J), on day 14. n = 10-11
515 mice per group. K-L, WT specific pathogen-free mice were fed the diets described in panel G for
516 7 days and feces were collected to measure the relative abundance of *L. johnsonii* by qRT-PCR
517 (K) and the ratio of cholic acid to taurocholic acid (CA:TCA) in fecal samples (L). n = 10-11 mice

518 per group. *P<0.05; **P<0.01; ***P<0.001; ****P<0.0001. Bar plots show mean and standard
519 deviation.
520
521 **Supplementary Figure Legends**
522 **Figure S1**. **Long-term beef protein feeding in specific pathogen free wild-type mice does**
523 **not induce signs of colitis.** Mice were fed chow, or purified diet containing beef protein (BP) or
524 pea protein (PP) isolate for 8 weeks. Disease activity index (DAI) was measured weekly (A) and
525 relative expression of *Tnfa* and *Il1b* was measured in colons at the end of the study (B). n = 6
526 mice per group. Bar plots show mean and standard deviation.
527
528 **Figure S2**. **Relative bacterial species abundance of individual mice fed beef or pea**
529 **protein-containing diets.** Species abundance in feces from individual mice is reported prior to
530 (A) and 7 days following (B) administration of diets containing beef protein (BP) or pea protein
531 (PP) isolate. Those species appearing in abundance <1% in all conditions are labeled as
532 'Other'.
533
534 **Figure S3. Dietary protein source does not affect goblet cell mucus quality.** C57BL/6J
535 mice were fed either beef protein (BP) or pea protein (PP)-containing diets for 7 days then
536 periodic acid Schiff staining was performed to quantify mucus quality within goblet cells.
537 Representative images (A) and quantification of staining (B) are shown. Bar plots show mean
538 and standard deviation.
539
540 **Figure S4**. **Taurocholic acid localizes to the colonic epithelium following oral**
541 **administration to mice.** C57BL/6J WT mice were administered daily oral gavage of PBS or
542 taurocholic acid (TCA) (0.35mg/kg) for 7 days and colon tissue sections were subjected to
543 MALDI-MSI to determine localization (A) and relative abundance (B) of TCA in each group. TCA

group is normalized to vehicle group in panel B. n = 4 samples per group. **P<0.01. Bar plots show mean and standard deviation.

Figure S5. **Psyllium supplementation protects against beef protein diet-induced worsening of DSS-induced colitis.** WT specific pathogen free mice were fed beef protein (BP) or pea protein (BP) diets containing cellulose or BP diet containing psyllium (BP + Psyllium) for 7 days. Mice were then administered 1% dextran sodium sulfate (DSS) and Disease Activity Index (DAI) was measured over 7 days (A) and colon length was measured on day 7 (B). Bar plots show mean and standard deviation.

References

1. Sartor RB, Wu GD. Roles for Intestinal Bacteria, Viruses, and Fungi in Pathogenesis of Inflammatory Bowel Diseases and Therapeutic Approaches. Gastroenterology. 2017;152(2):327-39.e4.
2. Perler BK, Friedman ES, Wu GD. The role of the gut microbiota in the relationship between diet and human health. Annual review of physiology. 2023;85:449-68.
3. Lee D, Albenberg L, Compher C, Baldassano R, Piccoli D, Lewis JD, et al. Diet in the Pathogenesis and Treatment of Inflammatory Bowel Diseases. Gastroenterology. 2015;148(6):1087-106.
4. Gleave A, Shah A, Tahir U, Blom J-J, Dong E, Patel A, et al. Using Diet to Treat Inflammatory Bowel Disease: A Systematic Review. Official journal of the American College of Gastroenterology | ACG. 2025;120(1).
5. Issokson K, Lee DY, Yarur AJ, Lewis JD, Suskind DL. The Role of Diet in Inflammatory Bowel Disease Onset, Disease Management, and Surgical Optimization. Official journal of the American College of Gastroenterology | ACG. 2025;120(1).
6. Hashash JG, Elkins J, Lewis JD, Binion DG. AGA Clinical Practice Update on Diet and Nutritional Therapies in Patients With Inflammatory Bowel Disease: Expert Review. Gastroenterology. 2024;166(3):521-32.
7. Kaplan GG, Ng SC. Understanding and Preventing the Global Increase of Inflammatory Bowel Disease. Gastroenterology. 2017;152(2):313-21.e2.
8. Kaplan GG, Windsor JW. The four epidemiological stages in the global evolution of inflammatory bowel disease. Nature Reviews Gastroenterology & Hepatology. 2021;18(1):56-66.
9. Kuenzig ME, Fung SG, Marderfeld L, Mak JWY, Kaplan GG, Ng SC, et al. Twenty-first Century Trends in the Global Epidemiology of Pediatric-Onset Inflammatory Bowel Disease: Systematic Review. Gastroenterology. 2022;162(4):1147-59.e4.
10. Daniel CR, Cross AJ, Koebnick C, Sinha R. Trends in meat consumption in the USA. Public Health Nutrition. 2011;14(4):575-83.

583 11. Al Hasan SM, Saulam J, Mikami F, Kanda K, Ngatu NR, Yokoi H, et al. Trends in per
584 Capita Food and Protein Availability at the National Level of the Southeast Asian Countries: An
585 Analysis of the FAO's Food Balance Sheet Data from 1961 to 2018. Nutrients. 2022;14(3).
586 12. Desai MS, Seekatz AM, Koropatkin NM, Kamada N, Hickey CA, Wolter M, et al. A
587 Dietary Fiber-Deprived Gut Microbiota Degrades the Colonic Mucus Barrier and Enhances
588 Pathogen Susceptibility. Cell. 2016;167(5):1339-53.e21.
589 13. Hryckowian AJ, Van Treuren W, Smits SA, Davis NM, Gardner JO, Bouley DM, et al.
590 Microbiota-accessible carbohydrates suppress Clostridium difficile infection in a murine model.
591 Nature Microbiology. 2018;3(6):662-9.
592 14. Llewellyn SR, Britton GJ, Contijoch EJ, Vennaro OH, Mortha A, Colombel J-F, et al.
593 Interactions Between Diet and the Intestinal Microbiota Alter Intestinal Permeability and Colitis
594 Severity in Mice. Gastroenterology. 2018;154(4):1037-46.e2.
595 15. Kostovcikova K, Coufal S, Galanova N, Fajstova A, Hudcovic T, Kostovcik M, et al. Diet
596 Rich in Animal Protein Promotes Pro-inflammatory Macrophage Response and Exacerbates
597 Colitis in Mice. Front Immunol. 2019;10.
598 16. Riva A, Kuzyk O, Forsberg E, Siuzdak G, Pfann C, Herbold C, et al. A fiber-deprived diet
599 disturbs the fine-scale spatial architecture of the murine colon microbiome. Nature
600 Communications. 2019;10(1):4366.
601 17. Montrose DC, Nishiguchi R, Basu S, Staab HA, Zhou XK, Wang H, et al. Dietary
602 Fructose Alters the Composition, Localization, and Metabolism of Gut Microbiota in Association
603 With Worsening Colitis. Cellular and Molecular Gastroenterology and Hepatology.
604 2021;11(2):525-50.
605 18. Neumann M, Steimle A, Grant ET, Wolter M, Parrish A, Willieme S, et al. Deprivation of
606 dietary fiber in specific-pathogen-free mice promotes susceptibility to the intestinal mucosal
607 pathogen Citrobacter rodentium. Gut Microbes. 2021;13(1):1966263.
608 19. Wolter M, Steimle A, Parrish A, Zimmer J, Desai Mahesh S. Dietary Modulation Alters
609 Susceptibility to Listeria monocytogenes and Salmonella Typhimurium with or without a Gut
610 Microbiota. mSystems. 2021;6(6):e00717-21.
611 20. Shan Y, Lee M, Chang EB. The Gut Microbiome and Inflammatory Bowel Diseases.
612 Annu Rev Med 2022;73:455-468.
613 21. Pereira GV, Boudaud M, Wolter M, Alexander C, De Sciscio A, Grant ET, et al.
614 Opposing diet, microbiome, and metabolite mechanisms regulate inflammatory bowel disease in
615 a genetically susceptible host. Cell Host & Microbe. 2024;32(4):527-42.e9.
616 22. Devkota S, Wang Y, Musch MW, Leone V, Fehlner-Peach H, Nadimpalli A, et al.
617 Dietary-fat-induced taurocholic acid promotes pathobiont expansion and colitis in Il10-/- mice.
618 Nature. 2012;487(7405):104-8.
619 23. Lloyd-Price J, Arze C, Ananthakrishnan AN, Schirmer M, Avila-Pacheco J, Poon TW, et
620 al. Multi-omics of the gut microbial ecosystem in inflammatory bowel diseases. Nature.
621 2019;569(7758):655-62.
622 24. Sinha SR, Haileselassie Y, Nguyen LP, Tropini C, Wang M, Becker LS, et al. Dysbiosis-
623 Induced Secondary Bile Acid Deficiency Promotes Intestinal Inflammation. Cell Host & Microbe.
624 2020;27(4):659-70.e5.
625 25. Yang ZH, Liu F, Zhu XR, Suo FY, Jia ZJ, Yao SK. Altered profiles of fecal bile acids
626 correlate with gut microbiota and inflammatory responses in patients with ulcerative colitis.
627 World J Gastroenterol. 2021:June 28;7(4):3609-29.
628 26. Joyce SA, Gahan CGM. Bile Acid Modifications at the Microbe-Host Interface: Potential
629 for Nutraceutical and Pharmaceutical Interventions in Host Health. Annual review of food
630 science and technology. 2016;7(1):313-33.
631 27. Gray SM, Moss AD, Herzog JW, Kashiwagi S, Liu B, Young JB, et al. Mouse adaptation
632 of human inflammatory bowel diseases microbiota enhances colonization efficiency and alters

633 microbiome aggressiveness depending on the recipient colonic inflammatory environment.
634 Microbiome. 2024;12(1):147.
635 28. Png CW, Lindén SK, Gilshenan KS, Zoetendal EG, McSweeney CS, Sly LI, et al.
636 Mucolytic Bacteria With Increased Prevalence in IBD Mucosa AugmentIn VitroUtilization of
637 Mucin by Other Bacteria. Official journal of the American College of Gastroenterology | ACG.
638 2010;105(11).
639 29. Seregin SS, Golovchenko N, Schaf B, Chen J, Pudlo NA, Mitchell J, et al. NLRP6
640 Protects Il10-/- Mice from Colitis by Limiting Colonization of Akkermansia muciniphila. Cell
641 Reports. 2017;19(4):733-45.
642 30. Sugihara K, Kitamoto S, Saraithong P, Nagao-Kitamoto H, Hoostal M, McCarthy C, et al.
643 Mucolytic bacteria license pathobionts to acquire host-derived nutrients during dietary nutrient
644 restriction. Cell Reports. 2022;40(3).
645 31. Hoek Kristen L, McClanahan Kathleen G, Latour Yvonne L, Shealy N, Piazuelo MB,
646 Vallance Bruce A, et al. Turicibacterales protect mice from severe Citrobacter rodentium
647 infection. Infect Immun. 2023;91(11):e00322-23.
648 32. Lynch JB, Gonzalez EL, Choy K, Faull KF, Jewell T, Arellano A, et al. Gut microbiota
649 Turicibacter strains differentially modify bile acids and host lipids. Nature Communications.
650 2023;14(1):3669.
651 33. Zhang W, Wang J, Zhang D, Liu H, Wang S, Wang Y, et al. Complete Genome
652 Sequencing and Comparative Genome Characterization of Lactobacillus johnsonii ZLJ010, a
653 Potential Probiotic With Health-Promoting Properties. Frontiers in Genetics. 2019;10.
654 34. Jia D-J-C, Wang Q-W, Hu Y-Y, He J-M, Ge Q-W, Qi Y-D, et al. Lactobacillus johnsonii
655 alleviates colitis by TLR1/2-STAT3 mediated CD206+ macrophagesIL-10 activation. Gut
656 Microbes. 2022;14(1):2145843.
657 35. Kastl A, Zong W, Gershuni VM, Friedman ES, Tanes C, Boateng A, et al. Dietary fiber-
658 based regulation of bile salt hydrolase activity in the gut microbiota and its relevance to human
659 disease. Gut Microbes. 2022;14(1):2083417.
660 36. Jantchou P, Morois S, Clavel-Chapelon F, Boutron-Ruault M-C, Carbonnel F. Animal
661 Protein Intake and Risk of Inflammatory Bowel Disease: The E3N Prospective Study. Official
662 journal of the American College of Gastroenterology | ACG. 2010;105(10).
663 37. Jowett SL, Seal CJ, Pearce MS, Phillips E, Gregory W, Barton JR, et al. Influence of
664 dietary factors on the clinical course of ulcerative colitis: a prospective cohort study. Gut.
665 2004;53(10):1479.
666 38. Lees CW, Gros B, Kyle JA, Plevris N, Derikx L, Constantine-Cooke N, et al. 477c
667 HABITUAL MEAT INTAKE IS ASSOCIATED WITH INCREASED RISK OF DISEASE FLARE IN
668 ULCERATIVE COLITIS: INITIAL RESULTS FROM THE PREDICCT STUDY. Gastroenterology.
669 2023;164(6):S-1571.
670 39. Jadhav A, Bajaj A, Xiao Y, Markandey M, Ahuja V, Kashyap PC. Role of Diet-
671 Microbiome Interaction in Gastrointestinal Disorders and Strategies to Modulate Them with
672 Microbiome-Targeted Therapies. Annu Rev Nutr. 2023;43:355-383.
673 40. Bibi S, De Sousa Moraes LF, Lebow N, Zhu M-J. Dietary Green Pea Protects against
674 DSS-Induced Colitis in Mice Challenged with High-Fat Diet. Nutrients. 2017;9(5).
675 41. Ahn E, Jeong H, Kim E. Differential effects of various dietary proteins on dextran sulfate
676 sodium-induced colitis in mice. Nutr Res Pract. 2022;16(6):700-15.
677 42. Chiang JYL, Ferrell JM. Bile Acids as Metabolic Regulators and Nutrient Sensors. Annu
678 Rev Nutr. 2019;39:175-200.
679 43. Kubota H, Ishizawa M, Kodama M, Nagase Y, Kato S, Makishima M, et al. Vitamin D
680 Receptor Mediates Attenuating Effect of Lithocholic Acid on Dextran Sulfate Sodium Induced
681 Colitis in Mice. International Journal of Molecular Sciences. 2023;24(4).

44. Abdel-Razek EA-N, Mahmoud HM, Azouz AA. Management of ulcerative colitis by dichloroacetate: Impact on NFATC1/NLRP3/IL1B signaling based on bioinformatics analysis combined with in vivo experimental verification. Inflammopharmacology. 2024;32(1):667-82.
45. Wolter M, Grant ET, Boudaud M, Pudlo NA, Pereira GV, Eaton KA, et al. Diet-driven differential response of Akkermansia muciniphila modulates pathogen susceptibility. Molecular Systems Biology. 2024;20(6):596-625-.
46. Larabi AB, Masson HLP, Bäumler AJ. Bile acids as modulators of gut microbiota composition and function. Gut Microbes. 2023;15(1):2172671.
47. van Best N, Rolle-Kampczyk U, Schaap FG, Basic M, Olde Damink SWM, Bleich A, et al. Bile acids drive the newborn's gut microbiota maturation. Nature Communications. 2020;11(1):3692.
48. Islam KBMS, Fukiya S, Hagio M, Fujii N, Ishizuka S, Ooka T, et al. Bile Acid Is a Host Factor That Regulates the Composition of the Cecal Microbiota in Rats. Gastroenterology. 2011;141(5):1773-81.
49. Tian YA-O, Gui W, Koo IA-O, Smith PB, Allman EA-O, Nichols RG, et al. The microbiome modulating activity of bile acids. Gut Microbes. 2020(Mar 5;11(4):979–996.).
50. Bretin A, Zou J, San Yeoh B, Ngo VL, Winer S, Winer DA, et al. Psyllium Fiber Protects Against Colitis Via Activation of Bile Acid Sensor Farnesoid X Receptor. Cellular and Molecular Gastroenterology and Hepatology. 2023;15(6):1421-42.
51. Sartor RB. Mechanisms of Disease: pathogenesis of Crohn's disease and ulcerative colitis. Nature Clinical Practice Gastroenterology & Hepatology. 2006;3(7):390-407.
52. Yang C, Merlin D. Unveiling Colitis: A Journey through the Dextran Sodium Sulfate-induced Model. Inflammatory Bowel Diseases. 2024;30(5):844-53.
53. Faith JJ, Ahern PP, Ridaura VK, Cheng J, Gordon JI. Identifying Gut Microbe–Host Phenotype Relationships Using Combinatorial Communities in Gnotobiotic Mice. Science Translational Medicine. 2014;6(220):220ra11-ra11.
54. Darfeuille-Michaud A, Neut C, Barnich N, Lederman E, Di Martino P, Desreumaux P, et al. Presence of adherent Escherichia coli strains in ileal mucosa of patients with Crohn's disease. Gastroenterology. 1998;115(6):1405-13.
55. Eun CS, Mishima Y, Wohlgemuth S, Liu B, Bower M, Carroll IM, et al. Induction of bacterial antigen-specific colitis by a simplified human microbiota consortium in gnotobiotic interleukin-10-/- mice. Infect Immun. 2014;82(6):2239-46.
56. Remke M, Groll T, Metzler T, Urbauer E, Kövilein J, Schnalzger T, et al. Histomorphological scoring of murine colitis models: A practical guide for the evaluation of colitis and colitis-associated cancer. Experimental and Molecular Pathology. 2024;140:104938.
57. Rath HC, Herfarth HH, Ikeda JS, Grenther WB, Hamm TE, Jr., Balish E, et al. Normal luminal bacteria, especially Bacteroides species, mediate chronic colitis, gastritis, and arthritis in HLA-B27/human beta2 microglobulin transgenic rats. J Clin Invest. 1996;98(4):945-53.
58. Chassaing B, Srinivasan G, Delgado MA, Young AN, Gewirtz AT, Vijay-Kumar M. Fecal Lipocalin 2, a Sensitive and Broadly Dynamic Non-Invasive Biomarker for Intestinal Inflammation. PLoS One. 2012;7(9):e44328.
59. Bai JDK, Saha S, Wood MC, Chen B, Li J, Dow LE, et al. Serine Supports Epithelial and Immune Cell Function in Colitis. The American Journal of Pathology. 2024;194(6):927-40.
60. Derrien M, van Baarlen P, Hooiveld G, Norin E, Muller M, de Vos W. Modulation of Mucosal Immune Response, Tolerance, and Proliferation in Mice Colonized by the Mucin-Degrader Akkermansia muciniphila. Front Microbiol. 2011;2.
61. Chetnik K, Benedetti E, Gomari DP, Schweickart A, Batra R, Buyukozkan M, et al. maplet: an extensible R toolbox for modular and reproducible metabolomics pipelines. Bioinformatics. 2022;38(4):1168-70.

DSS

A

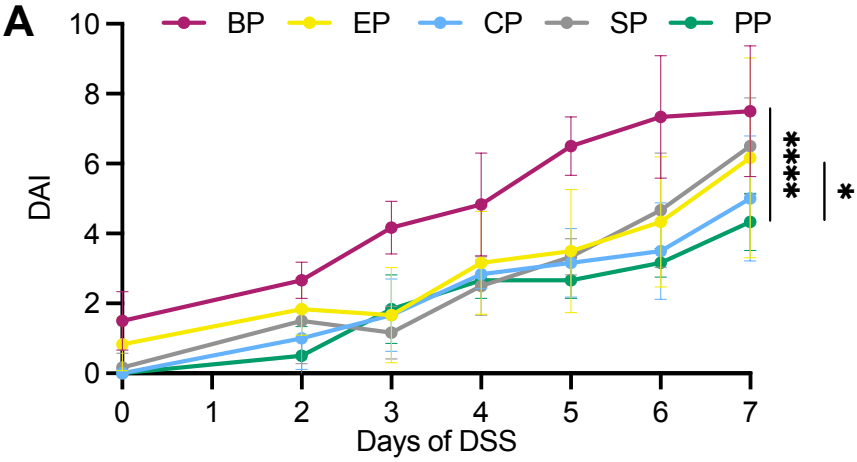

B

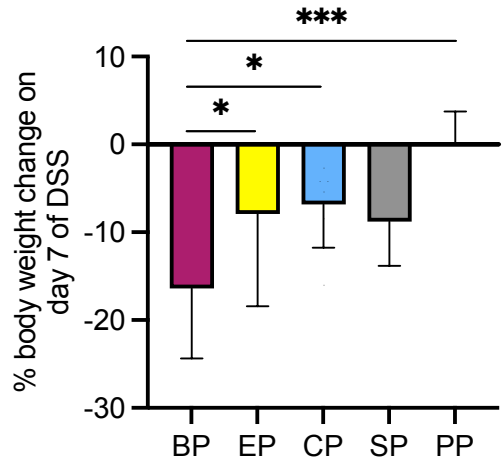

C

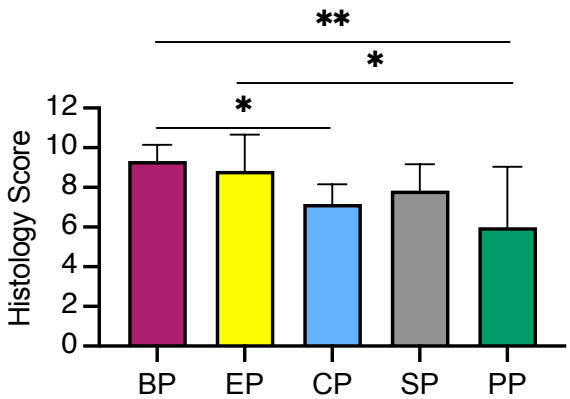

D

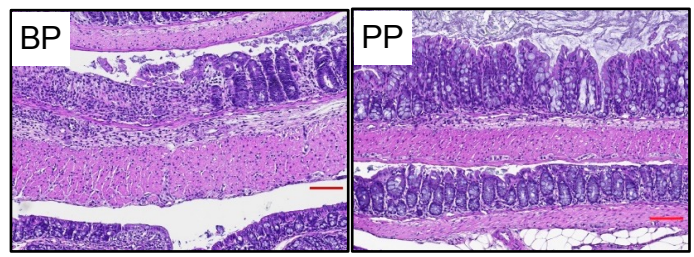

129.*Il10*$^{-/-}$ – IMM-HM2

E

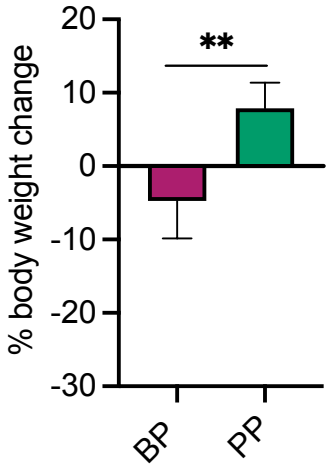

F

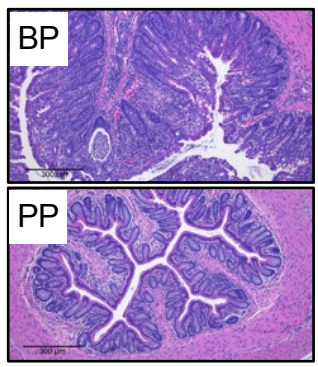

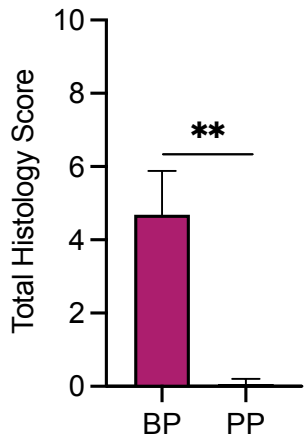

G

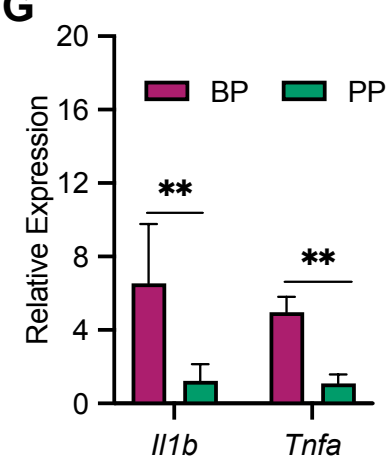

129.*Il10*$^{-/-}$ – IMM-g2

H

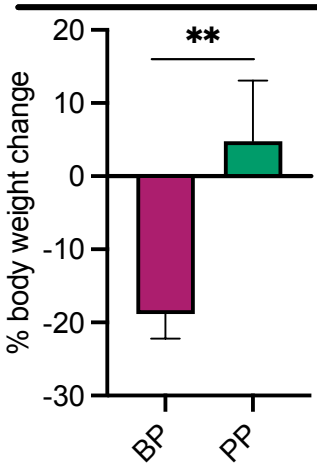

I

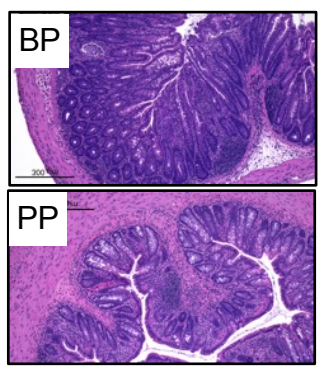

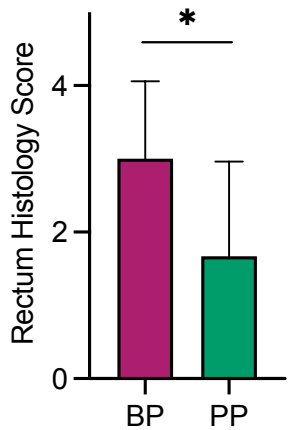

J

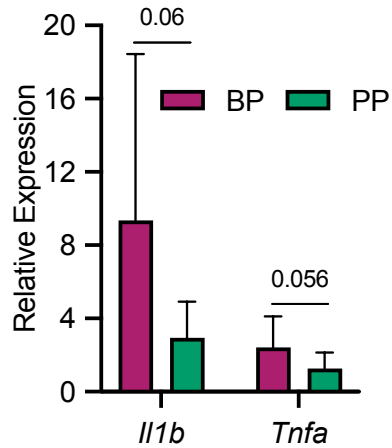

Figure 1

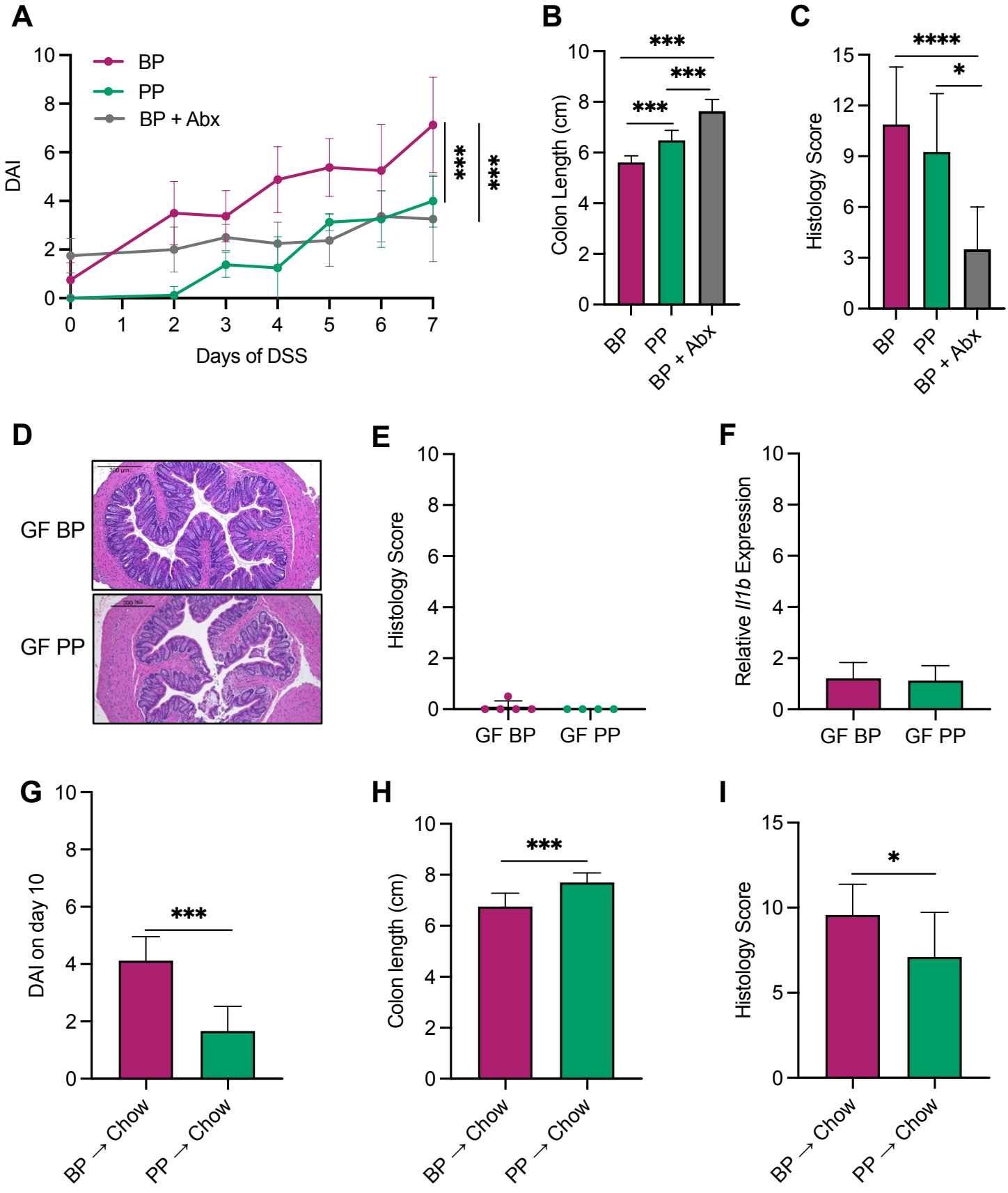
A
BP
PP
BP + Abx
DAI
Days of DSS
***
***
B
Colon Length (cm)
***
***
***
BP
PP
BP + Abx
C
Histology Score
****
*
BP
PP
BP + Abx
D
GF BP
GF PP
E
Histology Score
GF BP
GF PP
F
Relative Il1b Expression
GF BP
GF PP
G
DAI on day 10
***
BP → Chow
PP → Chow
H
Colon length (cm)
***
BP → Chow
PP → Chow
I
Histology Score
*
BP → Chow
PP → Chow

Figure 2

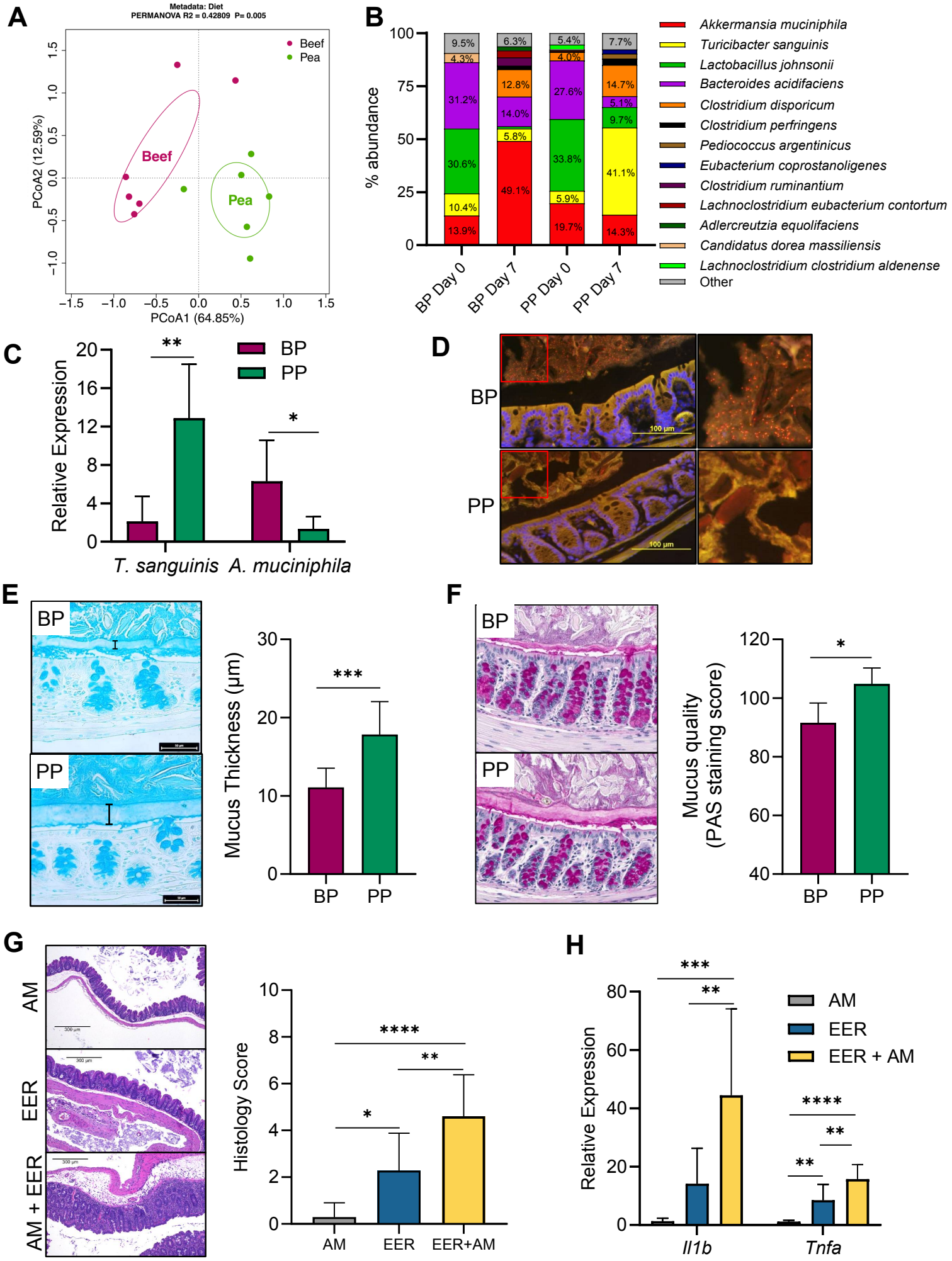
A
Metadata: Diet
PERMANOVA R2 = 0.42809 P= 0.005
Beef
Pea
PCoA2 (12.59%)
PCoA1 (64.85%)
B
% abundance
BP Day 0
BP Day 7
PP Day 0
PP Day 7
Akkermansia muciniphila
Turicibacter sanguinis
Lactobacillus johnsonii
Bacteroides acidifaciens
Clostridium disporicum
Clostridium perfringens
Pediococcus argentinicus
Eubacterium coprostanoligenes
Clostridium ruminantium
Lachnoclostridium eubacterium contortum
Adlercreutzia equolifaciens
Candidatus dorea massiliensis
Lachnoclostridium clostridium aldenense
Other
C
Relative Expression
BP
PP
T. sanguinis
A. muciniphila
D
BP
PP
100 µm
E
BP
PP
Mucus Thickness (µm)
F
BP
PP
Mucus quality
(PAS staining score)
G
AM
EER
AM + EER
Histology Score
AM
EER
EER+AM
H
Relative Expression
AM
EER
EER + AM
Il1b
Tnfa

Figure 3

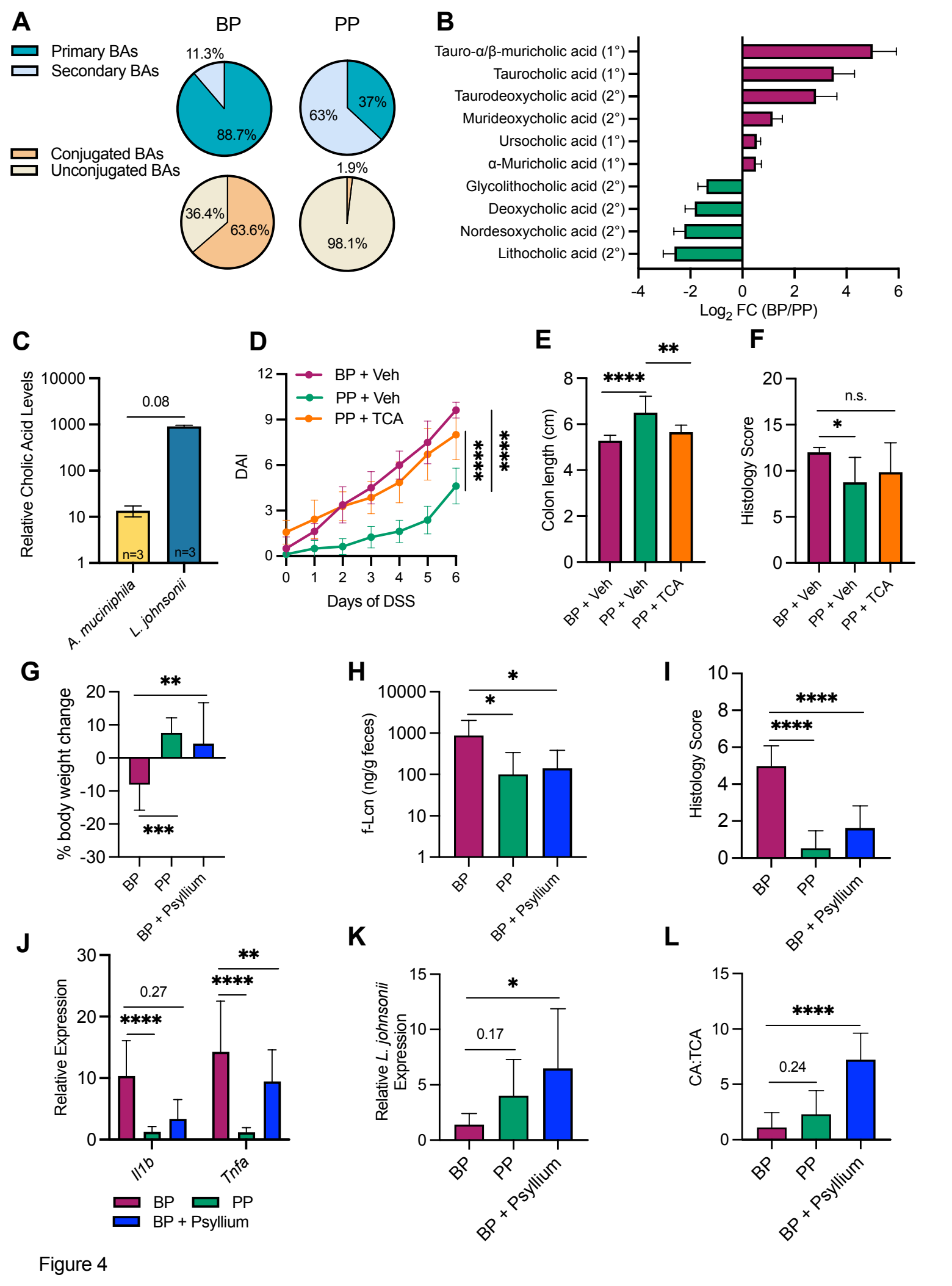
A
BP
PP
Primary BAs
Secondary BAs
11.3%
88.7%
63%
37%
Conjugated BAs
Unconjugated BAs
36.4%
63.6%
1.9%
98.1%
B
Tauro-α/β-muricholic acid (1°)
Taurocholic acid (1°)
Taurodeoxycholic acid (2°)
Murideoxycholic acid (2°)
Ursocholic acid (1°)
α-Muricholic acid (1°)
Glycolithocholic acid (2°)
Deoxycholic acid (2°)
Nordesoxycholic acid (2°)
Lithocholic acid (2°)
Log2 FC (BP/PP)
C
Relative Cholic Acid Levels
0.08
n=3
n=3
A. muciniphila
L. johnsonii
D
BP + Veh
PP + Veh
PP + TCA
DAI
Days of DSS
E
Colon length (cm)
BP + Veh
PP + Veh
PP + TCA
F
Histology Score
n.s.
G
% body weight change
BP
PP
BP + Psyllium
H
f-Lcn (ng/g feces)
I
Histology Score
J
Relative Expression
0.27
Il1b
Tnfa
BP
PP
BP + Psyllium
K
Relative L. johnsonii Expression
0.17
L
CA:TCA
0.24

Figure 4

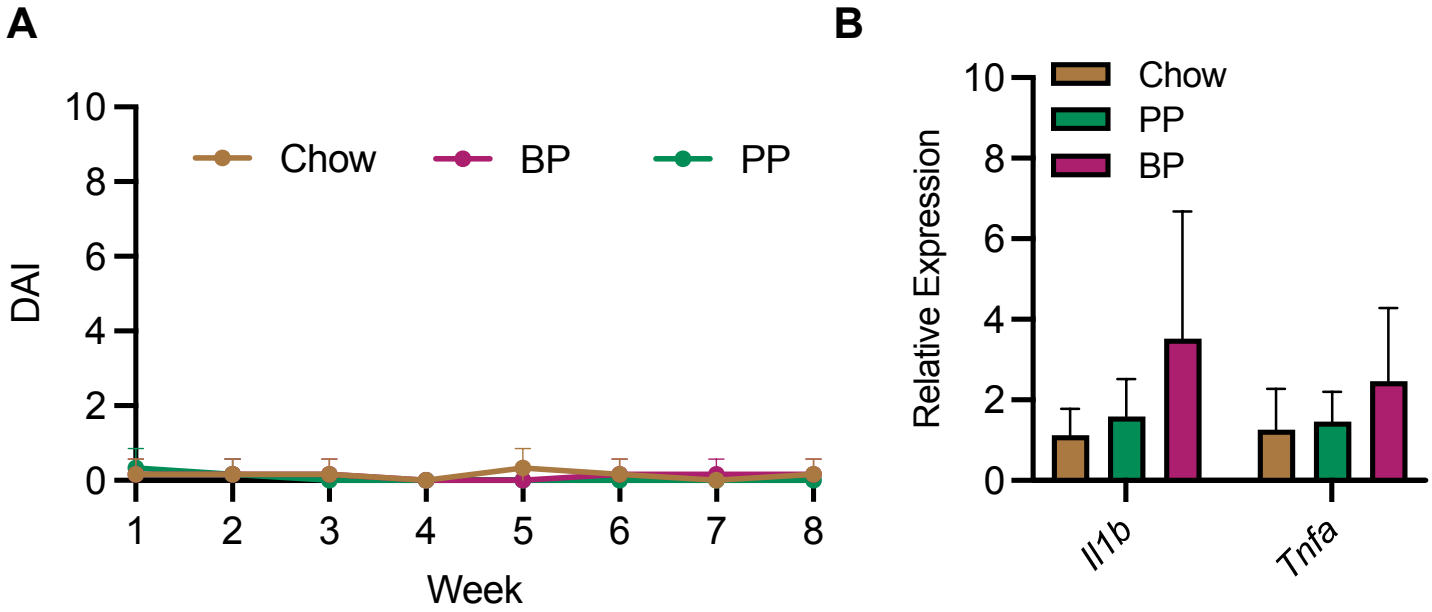

Figure S1

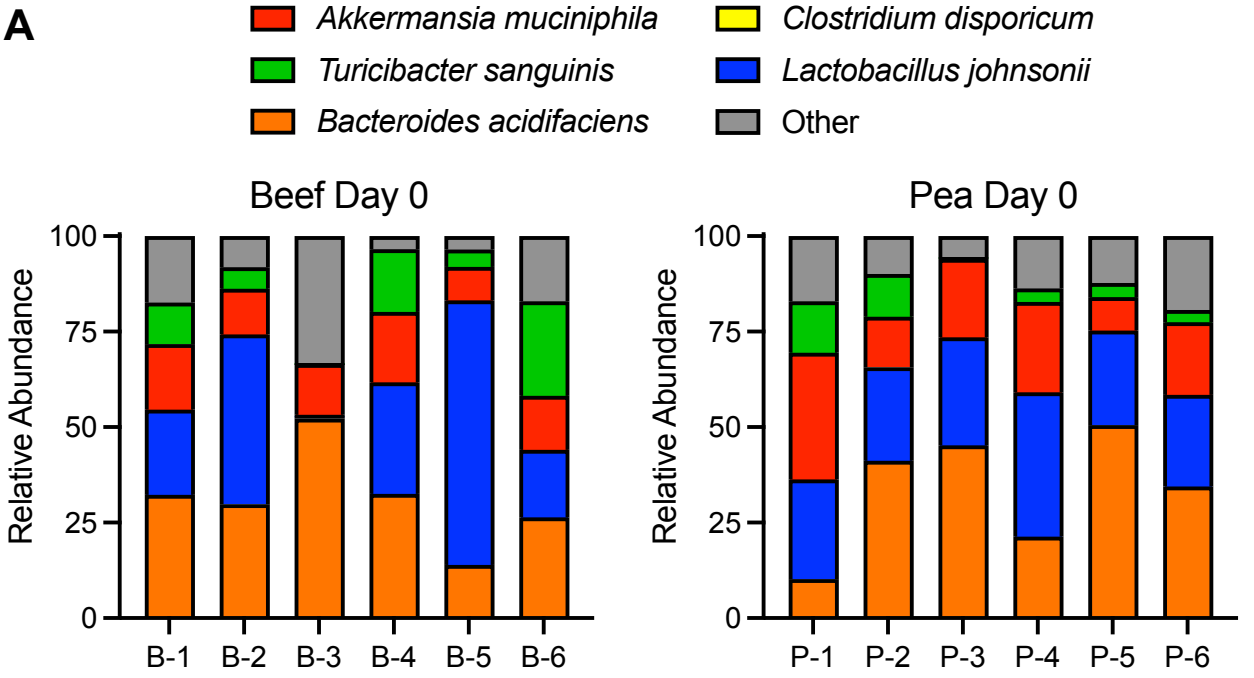
A
Akkermansia muciniphila
Clostridium disporicum
Turicibacter sanguinis
Lactobacillus johnsonii
Bacteroides acidifaciens
Other
Beef Day 0
Pea Day 0
Relative Abundance
100
75
50
25
0
B-1
B-2
B-3
B-4
B-5
B-6
P-1
P-2
P-3
P-4
P-5
P-6

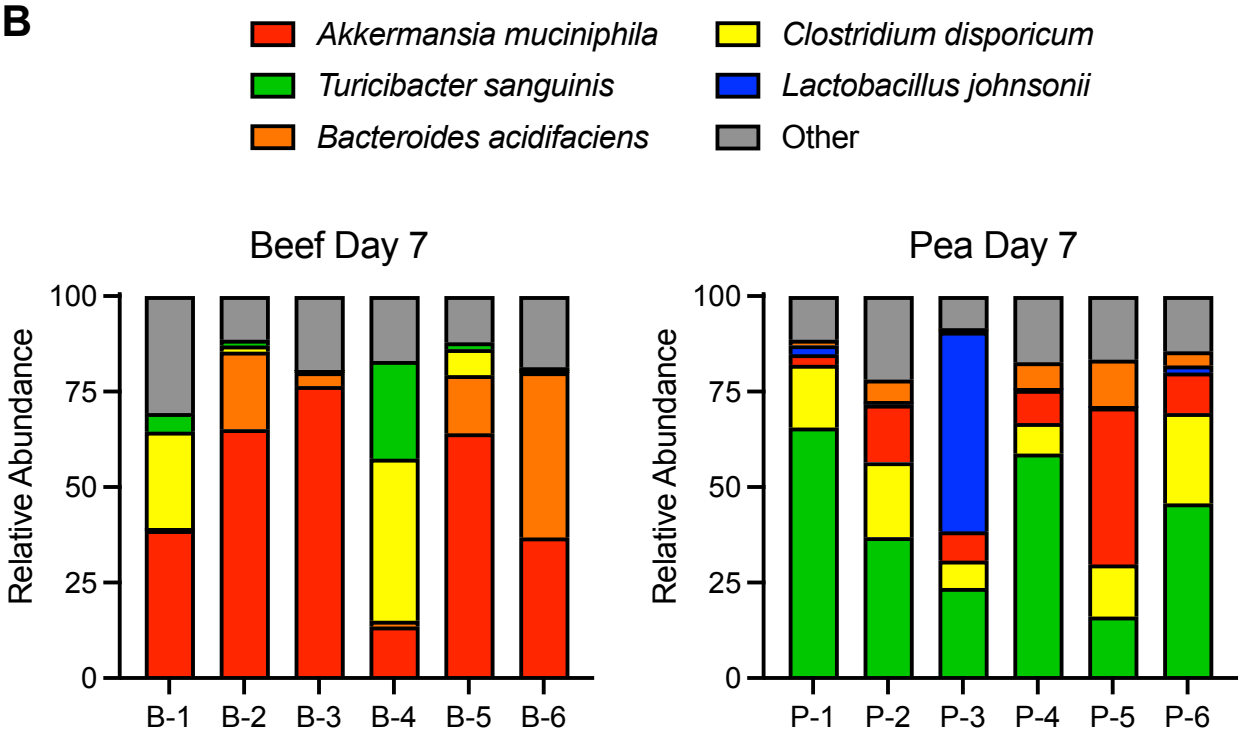
B
Akkermansia muciniphila
Clostridium disporicum
Turicibacter sanguinis
Lactobacillus johnsonii
Bacteroides acidifaciens
Other
Beef Day 7
Pea Day 7
Relative Abundance
100
75
50
25
0
B-1
B-2
B-3
B-4
B-5
B-6
P-1
P-2
P-3
P-4
P-5
P-6

Figure S2

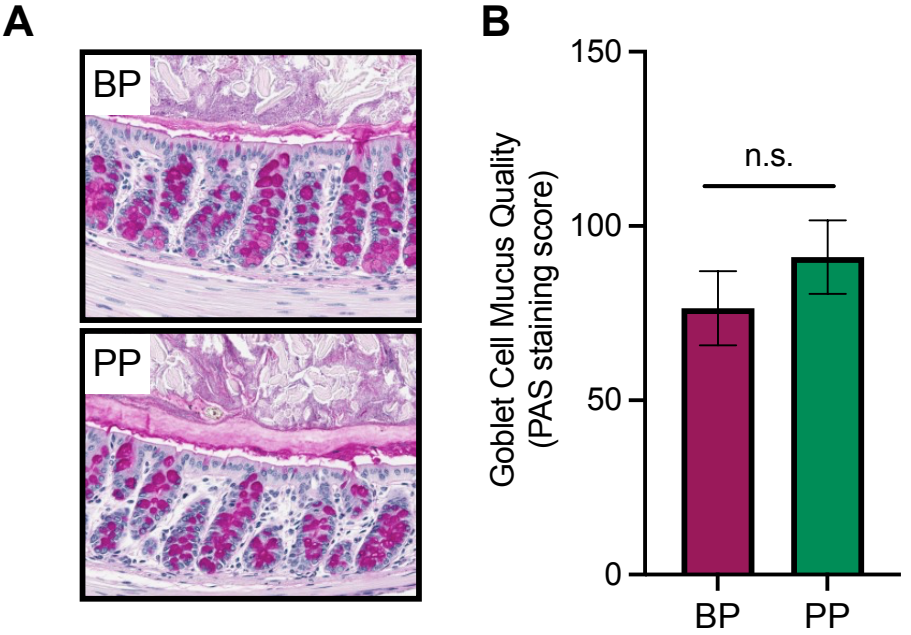
A
BP
PP
B
150
100
50
0
Goblet Cell Mucus Quality
(PAS staining score)
n.s.
BP
PP

Figure S3

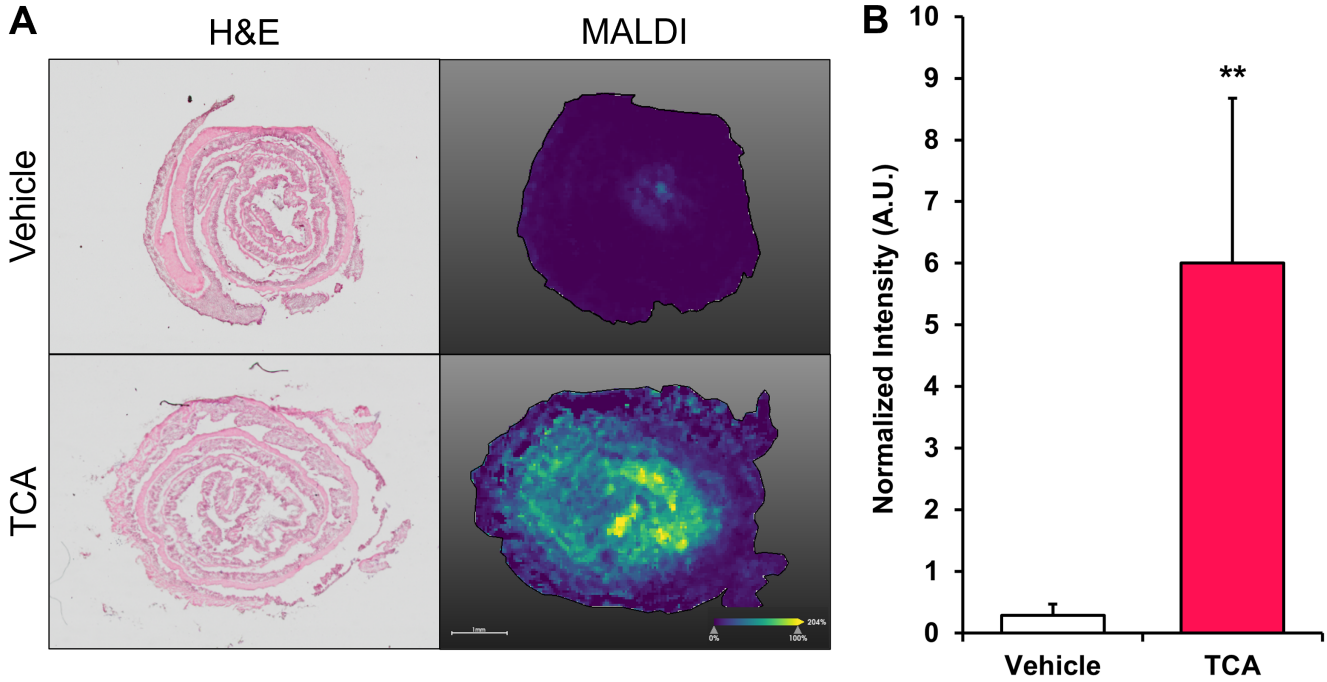
A
H&E
MALDI
Vehicle
TCA
B
Normalized Intensity (A.U.)
10
9
8
7
6
5
4
3
2
1
0
**
Vehicle
TCA

Figure S4

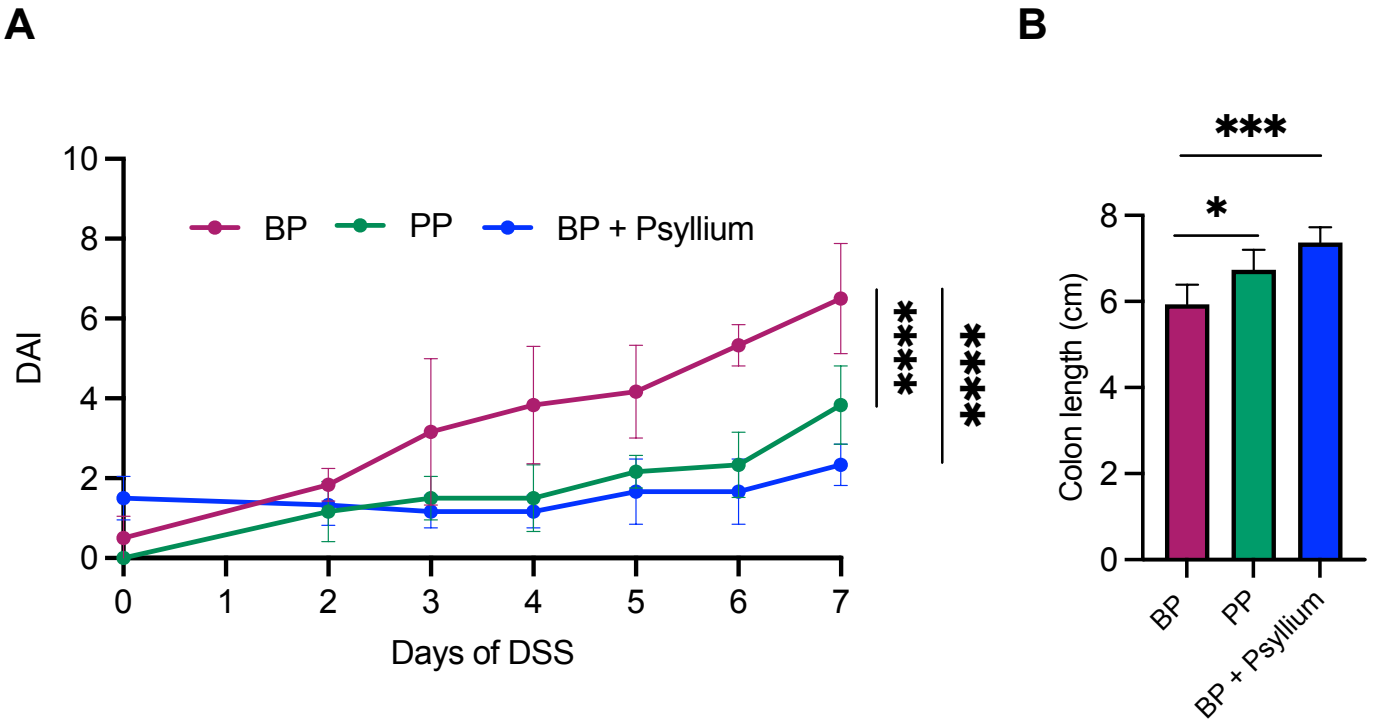
A
B
DAI
Days of DSS
BP
PP
BP + Psyllium
****
****
Colon length (cm)
***
*
BP
PP
BP + Psyllium

Figure S5

Table S1. Experimental Diet Formulations

	Beef	**Casein**	**Egg**	**Pea**	**Soy**	**Beef + Psyllium**
Ingredient	gm	gm	gm	gm	gm	gm
Casein	0	200	0	0	0	0
Soy Protein, Supro 661	0	0	0	0	202.3	0
Egg Whites	0	0	210.9	0	0	0
Beef Protein Isolate, Sigma	226.9	0	0	0	0	226.9
Pea Protein, Pure Bulk	0	0	0	209.1	0	0
L-Cystine	3	3	3	3	3	3
Corn Starch	398.486	397.486	389.286	398.486	395.486	385.329
Maltodextrin 10	132	132	132	132	132	132
Sucrose	100	100	100	100	100	100
Psyllium	0	0	0	0	0	52.63
Cellulose, BW200	50	50	50	50	50	0
Soybean Oil	70.8	70	70.2	51.8	63	70.8
t-Butylhydroquinone	0.014	0.014	0.014	0.014	0.014	0.014
Mineral Mix S10022G	0	0	0	0	0	0
Mineral Mix S10001A	17.5	17.5	17.5	17.5	17.5	17.5
Calcium Phosphate, Dibasic	17.5	17.5	17.5	17.5	17.5	17.5
Calcium Carbonate	0	0	0	0	0	0
Potassium Citrate, Monohydrate	0	0	0	0	0	0
Potassium Phosphate, Monobasic	0	0	0	0	0	0
Sodium Chloride	0	20.2	12.9	19.3	19.2	0
Vitamin Mix V10037	0	0	0	0	0	0
Vitamin Mix V10001	10	10	10	10	10	10
Biotin, 0.1%	0	0	0.4	0	0	0
Choline Bitartrate	2.5	2.5	2.5	2.5	2.5	2.5
Total	**1028.7**	**1020.2**	**1016.2**	**1011.2**	**1012.5**	**1018.2**
Protein (gm)	177.0	177.0	177.0	177.0	177.0	177.0
Carbohydrate (gm)	640.5	640.5	640.5	640.5	640.5	640.5
Fat (gm)	71.0	71.0	71.0	71.0	71.0	71.0
Fiber (gm)	50.0	50.0	50.0	50.0	50.0	52.63
Protein (kcal)	708.1	708.0	708.0	707.9	707.9	708.1
Carbohydrate (kcal)	2561.9	2561.9	2561.9	2561.9	2561.8	2561.9
Fat (kcal)	639.2	638.6	639.4	639.3	639.3	639.2
Total	3909.3	3908.6	3909.3	3909.2	3909.0	3909.3
Protein (gm%)	17.2	17.3	17.4	17.5	17.5	17.2
Carbohydrate (gm%)	62.3	62.8	63.0	63.3	63.3	63.0
Fat (gm%)	6.9	7.0	7.0	7.0	7.0	6.9
Protein (kcal%)	18.1	18.1	18.1	18.1	18.1	18.1
Carbohydrate (kcal%)	65.5	65.5	65.5	65.5	65.5	65.5
Fat (kcal%)	16.4	16.3	16.4	16.4	16.4	16.4
Sodium (g/kg)	8.8	8.8	8.8	8.8	8.8	8.8
kcal/gm	3.8	3.8	3.8	3.9	3.9	3.8

Table S2. Primer Sequences

Murine Targets		
Gene	Type	Sequence (5'-3')
B-actin	Forward	GGCTGTATTCCCCTCCATCG
	Reverse	CCAGTTGGTAACAATGCCATGT
Il1b	Forward	TGGGCCTCAAAGGAAAGAAT
	Reverse	CAGGCTTGTGCTCTGCTTGT
Tnfa	Forward	ACCCTCACACTCAGATCATCTTCTC
	Reverse	TGAGATCCATGCCGTTGG
Bacterial PCR Targets		
Akkermansia muciniphila	Akk-16S-F	GATAGTACCACAAGAGGAAGAGACG
	Akk-16S-R	TTCCCCCTCCATTACTCTAGTCTC
Lactobacillus johnsonii	Ljohn-16S-F	GCCTAGATGATTTTAGTGCTTGCAC
	Ljohn-16S-R	AGCAGAACCATCTTTCAAACTCTAGA
Turicibacter sanguinis	Turi-16S-F	TGTGACGGTACCTTATGAGAAAGC
	Turi-16S-R	GTTGACCAGTTTCCAATGACCCTC
Universal 16s Primer	Forward	ACTCCTACGGGAGGCAGCAG
	Reverse	ATTACCGCGGCTGCTGG
To amplify EER	Forward	U341F 5'-CCTACGGGRSGCAGCAG-3'
	Reverse	UA1406R 5'-ACGGGCGGTGWGTRCAA-3'